PHYSICAL REVIEW E **77**, 020301(R) (2008)

Interaction between intruders in vibrated granular beds

L. T. Lui, Michael R. Swift, R. M. Bowley, and P. J. King
School of Physics and Astronomy, University of Nottingham, Nottingham, NG7 2RD, United Kingdom
(Received 18 September 2007; published 20 February 2008)

Two neutrally buoyant intruder particles in a granular bed fluidized by vertical, sinusoidal vibration are known to interact with each other over a range of about five intruder diameters. Using molecular dynamics simulations, we investigate in detail the spatial and temporal nature of this interaction. We show that the force of attraction between intruders can be calculated from the local density and kinetic energy using a simple equation of state. Moreover, the interaction can be changed from attractive to repulsive by reducing the coefficient of restitution between the intruders and host particles, one of the key results of this work.

DOI: 10.1103/PhysRevE.77.020301 PACS number(s): 45.70.Mg

Granular materials are ubiquitous in nature and exhibit a wide range of nontrivial dynamical behavior [1]. Many industrial processes rely on the mixing or separation of these materials [2]. Understanding granular mixtures is an important scientific and technological challenge both to physicists and to engineers [3]. One key question is this: does a collection of intruder particles within a vertically vibrated bed segregate because the intruders are attracted to each other, or do they segregate because they congregate in a particular region of space? Insight into this question can be gained by studying the behavior of neutrally buoyant intruders in a vibrated granular bed. It has been shown, both in simulation [4,5] and experiment [6], that two intruders attract each other over a range of about five intruder diameters and that multiple intruders cluster.

In this communication, we investigate in detail the interaction mechanism between two neutrally buoyant intruders. We use two-dimensional (2D) molecular dynamics (MD) to determine how a single intruder modifies the bed around it, leading to local changes in the number density and kinetic energy of neighboring host particles. For two intruders which are close together, the changes in density and kinetic energy are enhanced between them, leading to a gradient in these quantities across each intruder. We use an approximate equation of state for the pressure as a function of the density and kinetic energy to determine the pressure difference across an intruder, so as to calculate the interaction at different times during a cycle. This calculated force is in very good agreement with the interaction force determined directly from molecular dynamics simulations. Finally, we show how the interaction can be modified by changing only the intruder-host coefficient of restitution.

Our simulations use molecular dynamics techniques to model the behavior of intruders in a vibrated granular bed [7]. We consider a 2D system of 1000 host particles, each disk having a diameter of 2 mm and a mass of 3 g, contained within a region of width 200 mm, corresponding to ten layers. Periodic boundary conditions in the horizontal direction are employed. The grains interact via a short range linear spring-dashpot force. The spring constant is taken to be 10^6 N m^{-1} and the dashpot damping parameter is chosen so that the coefficient of restitution is 0.9. The intruder particles have diameter 6 mm and a density equal to that of the host particles, so that they remain neutrally buoyant within the bed [4]. The intruder-intruder and intruder-host collisions also have a coefficient of restitution of 0.9. The system is subjected to vertical sinusoidal vibration at a frequency of 30 Hz and with a maximal vertical acceleration relative to gravity Γ, fixed at 3.6, as in Ref. [4].

We have run long computer simulations to determine how, on the average, intruders influence the bed around them. For each run we split the data into cycles, and within each cycle we collect data in 20 equally spaced time slices. For each time slice we divide space vertically and horizontally into 2 mm square pixels in the laboratory frame of reference. For each pixel, we can determine the number of host particles present and the total horizontal part of the kinetic energy. We simulate a few thousand seconds of the motion, and sample the data about 600 times each second. By averaging the data for a particular time slice we can obtain time-averaged values of the number of host particles in a pixel, $\bar{n}_0(x_i,z_i,k)$ and the corresponding horizontal part of the kinetic energy per pixel, $\bar{K}_0(x_i,z_i,k)$. Here, x_i and z_i are the coordinates of pixel i, for a particular time slice labeled by k, and the subscript 0 refers to the number of intruders present. The height of the base of the bed varies as $-A\cos(\omega t)$ so that the base is at its lowest position at $t=0$. A time slice labeled by k has phase $\omega t = 2\pi k/20$.

Under our vibratory conditions, the bed is thrown and lands once per cycle. When the bed lands a shock wave is created at the base of the cell; the wave propagates upwards and becomes more diffuse as it rises. This behavior has been studied in simulation [8], experiment [9], and through continuum modeling [10].

Once we have obtained $\bar{n}_0$ and $\bar{K}_0$ it is relatively straightforward to determine the *change* in the bed caused by adding a single neutrally buoyant intruder. The whole computation is repeated and the mean densities $\bar{n}_1(x_i,z_i,k)$ and kinetic energies per pixel $\bar{K}_1(x_i,z_i,k)$ are calculated *relative* to the instantaneous horizontal position of the intruder. Due to fluctuations the intruder may rise and fall by roughly three pixels.

The difference, $\Delta n_1 = \bar{n}_1(x_i,z_i,k) - \bar{n}_0(x_i,z_i,k)$, is a measure of how the density is affected around the intruder. Δn_1 is significant over a range of several intruder diameters, as is shown in Fig. 1 where we plot Δn_1 on a color (gray) scale as a function of position at five times during the cycle. It can be seen that around the intruder (shown as a dark blob) there is

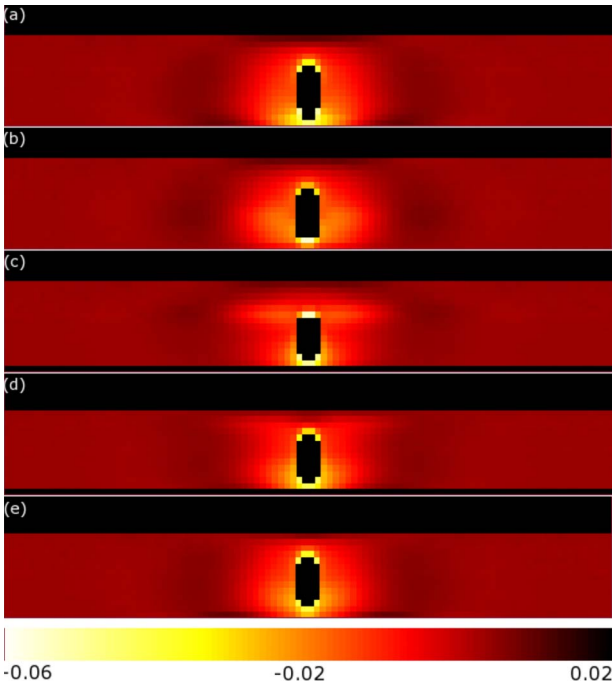

FIG. 1. (Color online) A series of figures showing Δn_1 (in units of host particles per square pixel) at different times in the cycle: (a) $k=0$, (b) $k=4$, (c) $k=8$, (d) $k=12$, and (e) $k=16$. For clarity only the lowest 15 layers are shown. The color scale at the bottom of the figure indicates the magnitude of Δn_1.

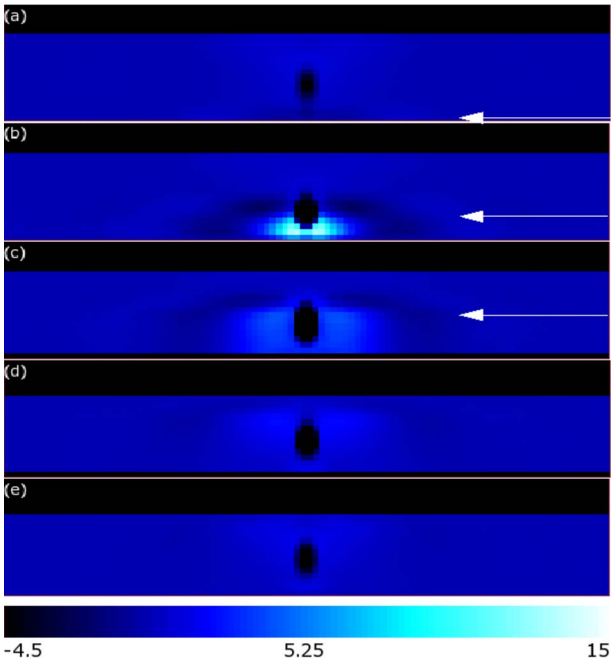

FIG. 2. (Color online) A series of figures showing ΔK_1 (in units of μJ per pixel) at different times in the cycle: (a) $k=0$, (b) $k=4$, (c) $k=8$, (d) $k=12$, and (e) $k=16$. The arrows indicate the vertical position of the shock wave. The color scale at the bottom of the figure indicates the magnitude of ΔK_1.

a slight decrease in the density (of around 5%) which is shown as a light halo which persists throughout the cycle. The horizontal range of the decrease is about three intruder diameters.

In Fig. 2 the variation in difference in kinetic energy per pixel, $\Delta K_1 = \bar{K}_1(x_i, z_i, k) - \bar{K}_0(x_i, z_i, k)$ is shown at five different times. ΔK_1 exhibits spatial and temporal fluctuations throughout a cycle. The arrows in the first three panels indicate the vertical height of the shock wave, defined by the position of the maximum of $-d\bar{K}_0/dz$ [9]. By a phase of $k=12$ the shock wave has largely dissipated. The positions of the arrows are correlated with the dark region passing the intruder.

Now we repeat the procedure for a system with two intruders which are free to move in the bed, but this time we bin the data according to the horizontal separation between the intruders, with the separation bin size taken to be an intruder diameter. The intruder on the left defines the center of the system; the horizontal distance of the intruder on the right defines the separation. As a result, the position of the intruder on the right appears somewhat blurred. In Fig. 3 we show the density difference Δn_2 when the separation between intruders lies in the range 3–4 intruder diameters. The low density regions around each intruder merge and create a larger low density area.

Figure 4 shows ΔK_2 for this system. In Fig. 4(a) we see that the value of ΔK_2 is negative in the region below the two intruders. In Fig. 4(b) the negative part of ΔK_2 travels upward and has just passed the intruders while below there is a region of positive ΔK_2. The value of ΔK_2 is more negative between the intruders than outside. In Fig. 4(c) the value of ΔK_2 is positive between the intruders and more positive than it is outside. Subsequently, ΔK_2 decreases as shown in Figs. 4(d) and 4(e). There is again a correlation between the tem-

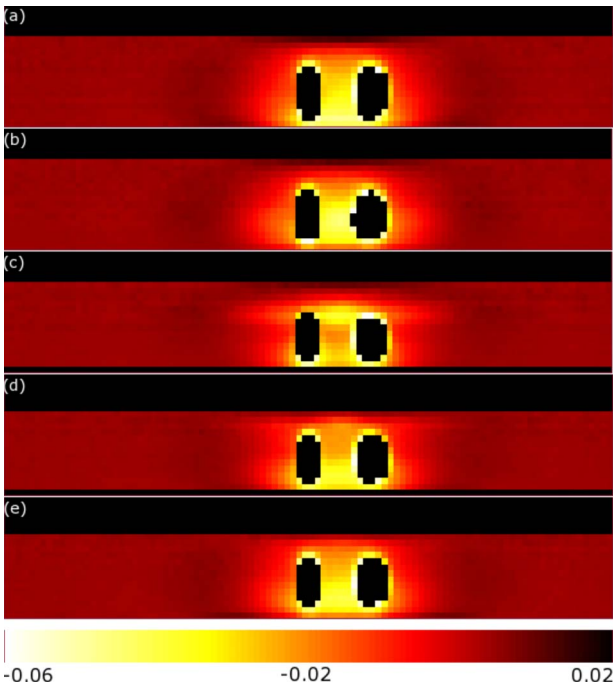

FIG. 3. (Color online) A series of figures showing Δn_2 (in units of host particles per square pixel) at different times in the cycle: (a) $k=0$, (b) $k=4$, (c) $k=8$, (d) $k=12$, and (e) $k=16$.

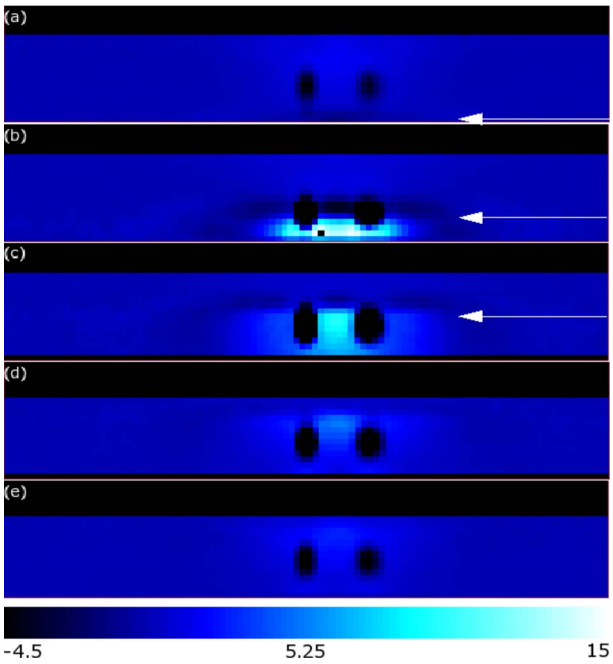

FIG. 4. (Color online) A series of figures showing ΔK_2 (in units of μJ per square pixel) at different times in the cycle: (a) $k=0$, (b) $k=4$, (c) $k=8$, (d) $k=12$, and (e) $k=16$. The arrows indicate the vertical position of the shock wave.

poral variation in ΔK_2 and the shock wave, shown by the arrows in Fig. 4.

The way in which two intruders modify the bed around them suggests the following very simple picture for the interaction. Each intruder generates a reduction in density around itself. When two intruders get sufficiently close to each other, the density reduction between them is enhanced. There is therefore a greater probability that the intruders will move towards each other than moving apart. Such a picture is similar in spirit to a depletion interaction [11]. However, this picture would suggest that the interaction between the intruders is always attractive at each phase of the cycle. In Fig. 5 we show the force on one intruder in the direction of the other as a function of phase throughout a cycle, calculated directly from the MD simulation. It can be seen that there is both attraction and repulsion during the cycle.

At the granular level, the intruders respond to collisions with the host particles. The corresponding course-grained description involves the pressure exerted by the bed on the intruders. In order to determine the pressure from the time-averaged density and kinetic energy fields that we have calculated, we need an equation of state. Recently, a simple equation of state has been proposed [12] and successfully used to explain the phase diagram of a dense, vertically vibrated bed of particles [13]. This equation of state is

$$P = 2\bar{K}\frac{n_c + \bar{n}}{n_c - \bar{n}}, \tag{1}$$

where $\bar{K}$ is the average kinetic energy density, $\bar{n}$ is the average number density, and n_c is the number density of hexagonal close packing.

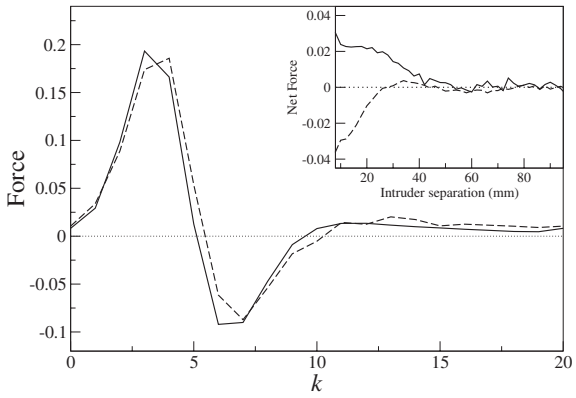

FIG. 5. The horizontal attractive force (in units of intruder particle weight) at different phases throughout a cycle, for intruders separated by 3–4 intruder diameters. The dashed line corresponds to the values measured in MD simulation, whereas the solid line shows the equivalent force determined from the equation of state, Eq. (1). The inset shows the average force over a cycle for a system with host-intruder restitution 0.9 (solid line) and 0.7 (dashed line). The latter curve shows that the net intruder interaction is repulsive.

Here we use this equation of state to estimate the pressure field around and between the intruders. From the pressure field, we can determine the resulting force on the intruders at each point in the cycle. To do this we calculated the difference in pressure between the pixel just on the left and just on the right of the left intruder. To determine the corresponding force, we simply multiply the pressure by the diameter of an intruder, ignoring any geometrical factors. This force can then be compared to the force calculated directly from intruder-host collisions. Figure 5 shows a comparison between the force determined from the pressure (solid line) and equivalent force from the MD simulation (broken line) over a complete cycle, for intruders separated by 3–4 intruder diameters. The agreement is remarkably good, given the approximate nature of the pressure calculation. Similar agreement is obtained for other intruder separations.

The good agreement indicates that we can understand the interaction between intruders by considering the time-averaged density and kinetic energy around the intruders. When ΔK_2 is negative between the intruders [Fig. 4(b)] the gradient of ΔK_2 in the horizontal direction leads to an attraction. Later in the cycle, ΔK_2 is positive between the intruders [Fig. 4(c)] and the gradient of ΔK_2 in the horizontal direction leads to a repulsion. This temporal variation of the force throughout a cycle results from the propagation of the shock wave.

The shock wave contains a peak in kinetic energy which propagates upwards through the bed. Huang *et al.* [9] have shown that the speed of the shock wave increases monotonically with an increase in the number density. It follows that in the lower density region between the intruders the shock wave moves slightly more slowly than it does elsewhere, leading to a retardation of the vertical position of the peak. Early in the cycle, the kinetic energy is greater outside the intruders than between them; later in the cycle the reverse is true. Consequently, there is a gradient in kinetic energy which leads to attraction early in the cycle and repulsion

later on. The corresponding pressure is enhanced by the density approaching the critical density early in the cycle. Once the shock wave has passed, the pressure difference tends to zero.

Finally, we address the question of why there is a reduced density around each intruder. In the simulations described so far, the coefficient of restitution is the same for host-host, intruder-intruder, and host-intruder collisions. If the intruder were replaced by a loosely packed group of seven host particles, corresponding approximately to the same areal density, there would be extra dissipation due to inelastic collisions between these particles. Consequently, the host particles in the immediate neighborhood of the intruder are slightly more energetic than elsewhere, because the intruder does not dissipate as much energy as an equivalent collection of host particles. The greater kinetic energy of host particles immediately around the intruders acts to push host particles away from the intruder, leading to a decrease in density close to the intruder and a slight excess in density further away, as shown in Fig. 1.

As a test of this idea, we have repeated the above simulations for a system in which the host-intruder and intruder-intruder collisions have a coefficient of restitution of 0.7, while keeping the host-host restitution coefficient at 0.9. All other system parameters remain the same. The simulations show that there is no longer a significant density reduction around a single intruder. This in turn modifies the interaction between two intruders; there is a reduction in the attractive force early in the cycle and an increase in the repulsive part, leading to a net repulsive force when averaged over a cycle, shown in the inset to Fig. 5. If simulations are run with multiple intruders, we observe no clustering if the intruder-host restitution is 0.7, whereas the system strongly clusters if the coefficients of restitution are all 0.9 [4].

Finally, let us consider the effects of changing either the bed depth or Γ. If the bed is sufficiently deep, the granular Leidenfrost effect occurs [13], which prevents the intruders from moving freely around the bed. Similarly, for sufficiently low values of Γ, the bed is insufficiently agitated to allow the intruders to diffuse freely. In both cases the intruders do not interact. For the bed depth of ten layers considered above, increasing Γ from 3.6 to 6 reduces the overall strength of the interaction. There is still a shock wave present but the timing of the attractive and repulsive parts are slightly delayed and the attractive part is slightly weakened. Nevertheless, as at lower values of Γ, reducing the coefficient of restitution to 0.7 still turns the attraction into a repulsion.

[1] H. M. Jaeger, S. R. Nagel, and R. P. Behringer, Rev. Mod. Phys. **68**, 1259 (1996).
[2] B. A. Wills, *Mineral Process Technology*, 6th ed. (Butterworth and Heinmann, Boston, 1997).
[3] For a review, see A. Kudrolli, Rep. Prog. Phys. **67**, 209 (2004), and references therein.
[4] D. A. Sanders, M. R. Swift, R. M. Bowley, and P. J. King, Phys. Rev. Lett. **93**, 208002 (2004).
[5] L. T. Lui, M. R. Swift, R. M. Bowley, and P. J. King, Phys. Rev. E **75**, 051303 (2007).
[6] D. A. Sanders *et al.*, Europhys. Lett. **73**, 349 (2006).
[7] For a review, see H. J. Herrmann and S. Luding, Continuum Mech. Thermodyn. **10**, 189 (1998).
[8] J. Bougie, Sung Joon Moon, J. B. Swift, and H. L. Swinney, Phys. Rev. E **66**, 051301 (2002).
[9] K. Huang, G. Miao, P. Zhang, Y. Yun, and R. Wei, Phys. Rev. E **73**, 041302 (2006).
[10] A. Goldshtein *et al.*, J. Fluid Mech. **287**, 349 (1995).
[11] M. Dijkstra, R. van Roij, and R. Evans, Phys. Rev. E **59**, 5744 (1999), and references therein.
[12] E. L. Grossman, T. Zhou, and E. Ben-Naim, Phys. Rev. E **55**, 4200 (1997).
[13] P. Eshuis, K. van der Weele, D. van der Meer, and D. Lohse, Phys. Rev. Lett. **95**, 258001 (2005).